Terahertz dielectric properties of high-resistivity single-crystal ZnO

Abul K. Azad
School of Electrical and Computer Engineering, Oklahoma State University, Stillwater, Oklahoma 74078

Jiaguang Han
Shanghai Institute of Applied Physics, Chinese Academy of Sciences, Shanghai 201800, People's Republic of China and High Energy Accelerator Research Organization, Tsukuba, Ibaraki 305-0801, Japan

Weili Zhang[a)]
School of Electrical and Computer Engineering, Oklahoma State University, Stillwater, Oklahoma 74078

(Received 9 August 2005; accepted 17 November 2005; published online 11 January 2006)

We present experimental characterization of complex dielectric properties of high-resistivity single-crystal ZnO by terahertz time-domain spectroscopy in the frequency range extending from 0.3 to 3.5 THz. The measured refractive index, power absorption, and dielectric function are well fit by the pseudo-harmonic model of dielectric response. In addition, from the extrapolation of the experimental results, we show that the absorption is dominated by the transverse optical (TO) E_1 phonon mode centered at frequency $(\omega_{TO}/2\pi)$ 12.42 THz. © *2006 American Institute of Physics*. [DOI: 10.1063/1.2164903]

Zinc oxide (ZnO), a wide-band-gap II-VI semiconductor, has attracted enormous attention because of potential applications in electro-optic, acousto-optic, and optoelectronic devices. A direct band gap of 3.37 eV (Ref. 1) at room temperature makes ZnO one of the most promising semiconductors for photonic devices in the ultraviolet range.[2,3] With proper doping, ZnO can be made electrically conductive and transparent in the visible spectral region such that it can be used as the transparent conductive electrodes in solar cells and flat panel displays.[4] It has also been demonstrated experimentally that ZnO shows significantly higher radiation hardness than Si, GaN, and GaAs.[5] Additionally, the large excitonic binding energy of about 60 meV, which is stable at room temperature, makes ZnO a possible candidate for the room-temperature polariton lasers.[6] The infrared dielectric function and the optical phonon modes of highly resistive single-crystal ZnO were investigated using ellipsometry and Raman scattering techniques over the frequency range from 300 to 1200 cm^{-1}.[4]

Recently, pulsed terahertz radiation has been demonstrated from a photoconductive switch fabricated on high-resistivity single-crystal ZnO.[7] ZnO is considered as a promising material for terahertz optics because of a number of advantages: Ease in fabrication, wide band gap, rather high mobility and resistivity, and transparency in a broad frequency range. The experimental result indicated that the high breakdown electric field enables ZnO to be an intriguing semiconductor in high-power terahertz generation. It is essential to explore the detailed optical and dielectric properties of ZnO in the broad terahertz frequency region. In this letter, the far-infrared optical properties and the complex dielectric function of high-resistivity single-crystal ZnO are experimentally characterized by use of terahertz time-domain spectroscopy (THz-TDS). The measured refractive index, power absorption, and complex dielectric function are compared with the pseudo-harmonic model. In the scope of our frequency range from 0.3 to 3.5 THz, the experimental data agree well with theoretical fitting. The measured power absorption, which increased approximately quadratically with frequency, was found to be dominated by the transverse optical (TO) E_1 phonon at frequency $(\omega_{TO}/2\pi)$ 12.42 THz.

The ZnO sample is an undoped 5 mm × 5 mm × 0.5-mm-thick freestanding single crystal (obtained from MTI Corporation, USA). The both-side polished sample has crystal orientation ⟨0001⟩ with *c*-axis perpendicular to the surface. Hydrothermal growth method was used to fabricate the wurtzite high-resistivity ZnO with purity higher than 99.99%. The ZnO crystal was characterized with a photoconductive switch-based THz-TDS system which has an 8-F configuration and an useable bandwidth extending from 0.1 to 4.5 THz as described elsewhere.[8,9] The ZnO sample is attached to a mechanical holder and has a 4.5-mm-diameter optical aperture, while another identical clear hole is used as a reference. Both the sample and reference are centered over the 3.5-mm terahertz beam waist alternatively in order to ensure the entire frequency component passing through the sample and reference.

The transmitted electric field of terahertz pulses through the sample and the reference are recorded in time domain and the corresponding frequency spectra are obtained by numerical Fourier transform. Due to the limited thickness of the ZnO crystal, the main transmitted terahertz pulse through the sample is trailed by multiple-reflected pulses in time domain. However, the clean separation between the main transmitted pulse and the first internal reflection enables us to perform data analysis on the main pulse only. The measured reference and sample pulses and the corresponding spectra are shown in Fig. 1. In order to increase the signal-to-noise ratio, every pulse curve is the average of seven individual measurements. The complex spectrum of the transmitted sample pulse $E_{sam}(\omega)$ can be extrapolated in terms of reference spectrum $E_{ref}(\omega)$ and the transfer function as[10]

$$\frac{E_{sam}(\omega)}{E_{ref}(\omega)} = t_{12}t_{21}e^{iL(k-k_0)}e^{-\alpha L/2}, \tag{1}$$

where t_{12} and t_{21} are the frequency-dependent complex Fresnel transmission coefficients, L is the thickness of the sample, α is the power absorption, and $k=2\pi n_r/\lambda$ and k_0

a)Electronic mail: wwzhang@okstate.edu

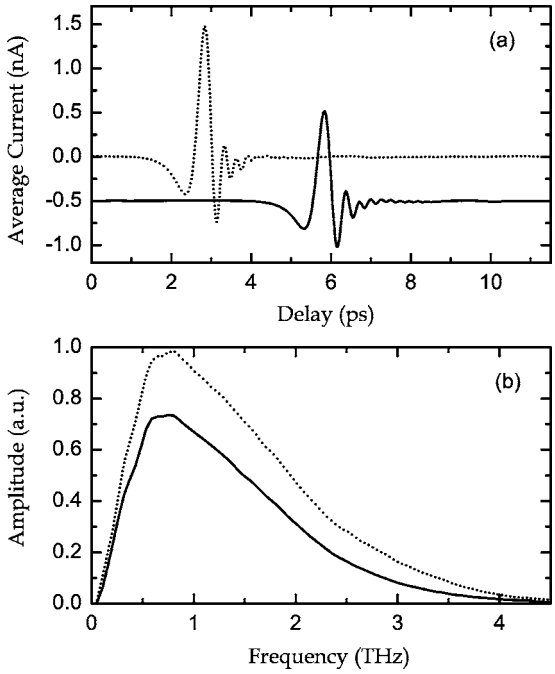

FIG. 1. (a) Measured THz pulses transmitted through reference (dotted line) and sample (solid line). For clarity, the sample pulse is vertically displaced by −0.5 nA. (b) Corresponding amplitude spectra of the measured reference pulse (dotted line) and sample pulse (solid line).

$=2\pi/\lambda$ are the propagation wave vectors. Based on this relation, the frequency-dependent power absorption $\alpha(\omega)$ and the refractive index $n(\omega)$ of the ZnO crystal can be directly determined by the measured data quite accurately.

The experimentally extracted power absorption $\alpha(\omega)$ and the refractive index $n(\omega)$ of single-crystal ZnO are plotted in Fig. 2 over the frequency region from 0.3 to 3.5 THz. The power absorption increases with increasing frequency and no prominent absorption peaks are observed below

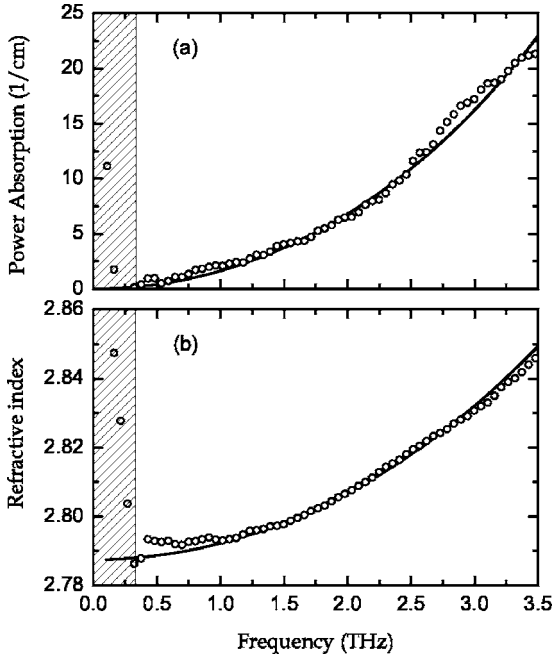

FIG. 2. (a) Comparison of measured power absorption α (open circles) with that obtained from pseudo-harmonic theoretical fitting (solid line). (b) Measured refractive index (open circles) and the theoretical fitting (solid line).

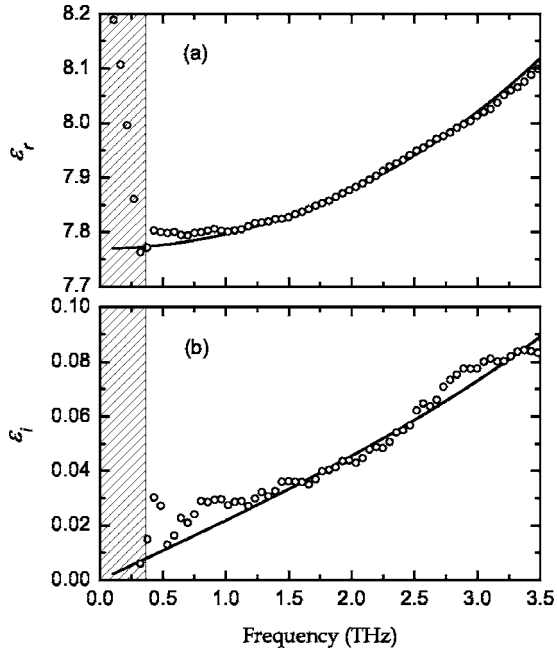

FIG. 3. Complex dielectric constant of single-crystal ZnO: (a) measured real part of dielectric constant ε_r (open circles) and the theoretical fitting (solid line); (b) measured imaginary dielectric constant ε_i (open circles) and the theoretical fitting (solid line).

3.5 THz. This can be verified by the measured refractive index which shows no remarkable features. Employing the measured data of power absorption and refractive index, we obtain the frequency-dependent complex dielectric function through the relation: $\varepsilon(\omega)=(n_r+in_i)^2$, where the imaginary part of the refractive index n_i is related to the power absorption as $n_i=\alpha\lambda/4\pi$. Hence, the real and the imaginary part of the dielectric constant are determined as $\varepsilon_r=n_r^2-(\alpha\lambda_0/4\pi)^2$ and $\varepsilon_i=\alpha n_r\lambda_0/2\pi$. The open circles shown in Fig. 3 represent the recorded data of the complex dielectric constant. In Fig. 3(a), the real dielectric constant shows a feature that is essentially the square of the refractive index n_r because the absorption by the sample is small in the spectral region concerned and the contribution of the absorption coefficient to the real dielectric constant is nearly negligible. The imaginary dielectric constant plotted in Fig. 3(b) shows proportional feature to the dielectric loss of the resonance process.

Generally, optical absorption of ionic crystals in the far-infrared terahertz region is attributed to the lattice vibrations. The interaction of a radiation field with the fundamental lattice vibration results in absorption of electromagnetic wave due to the creation or annihilation of lattice vibration. In the frame of the classical theory of independent pseudo-harmonic approximation, such process can be described below, considering the phonon contribution to the dielectric function[11]

$$\varepsilon(\omega)=\varepsilon_\infty+\frac{(\varepsilon_0-\varepsilon_\infty)\omega_{\mathrm{TO}}^2}{\omega_{\mathrm{TO}}^2-\omega^2-i\gamma\omega}, \tag{2}$$

where ε_∞ is the high-frequency dielectric constant, ε_0 is the low-frequency dielectric constant, ω_{TO} is the frequency of the TO phonon mode, and γ is the damping constant. Equation (2) can be written as a set of separate equations for the real and the imaginary part of the frequency-dependent dielectric function as

$$\varepsilon(\omega) = \varepsilon_r(\omega) + i\varepsilon_i(\omega), \tag{3}$$

with

$$\varepsilon_r(\omega) = \varepsilon_\infty + \frac{(\varepsilon_0 - \varepsilon_\infty)(\omega_{\mathrm{TO}}^2 - \omega^2)\omega_{\mathrm{TO}}^2}{(\omega_{\mathrm{TO}}^2 - \omega^2)^2 + \gamma^2\omega^2}, \tag{4}$$

$$\varepsilon_i(\omega) = \frac{(\varepsilon_0 - \varepsilon_\infty)\omega\gamma\omega_{\mathrm{TO}}^2}{(\omega_{\mathrm{TO}}^2 - \omega^2)^2 + \gamma^2\omega^2}. \tag{5}$$

Three parameters are used to fit the experimental data: $\varepsilon_0 = 7.77$, $\omega_{\mathrm{TO}}/2\pi = 12.42$ THz, and $\gamma/2\pi = 0.82$ THz. Given the high-frequency dielectric constant $\varepsilon_\infty = 3.705$,[12] the frequency-dependent complex dielectric constant is obtained from Eqs. (3)–(5). This theoretical calculation presents well fit on the data measured by THz-TDS, as shown in Figs. 2 and 3.

The good agreement between the experimental data and the fitting indicates the presence of a dominant TO-phonon resonance centered at $\omega_{\mathrm{TO}}/2\pi = 12.42$ THz with a linewidth of $\gamma/2\pi = 0.82$ THz and a strength $\varepsilon_{\mathrm{st}} = \varepsilon_0 - \varepsilon_\infty = 4.065$. It is worth noting that such a TO phonon resonance agrees well with the previous measurements.[13–16] As one of the II-VI compounds, wurtzite ZnO belongs to the $C_{6v}^4(P6_3mc)$ space group. There are 4 atoms per unit cell leading to 12 phonon branches: 9 optical and 3 acoustic. Group theory predicts the existence of the following optical modes:[17–19] an A_1 branch, an E_1 branch, two E_2 branches and two silent B_1 modes. The A_1 and E_1 are both Raman active and infrared active, while E_2 is Raman active only. In addition, the infrared-active A_1 and E_1 branches split into longitudinal optical (LO) and transverse optical component. The previous IR reflectivity measurement found the frequency of the TO (E_1) at 414 cm^{-1} (12.42 THz),[16] and the later Raman spectrum also observed such a TO (E_1) located at 413 cm^{-1} (12.40 THz).[13] The extrapolation based on the fitting of our experimental results gives a better agreement with this typical value.

Furthermore, our result is confirmed by the estimation of the frequency of LO (E_1). It is known that the frequency of LO (E_1) can be estimated from the well-known Lyddane–Schs–Teller relationship, $\omega_{\mathrm{LO}}^2/\omega_{\mathrm{TO}}^2 = \varepsilon_0/\varepsilon_\infty$. Using the above fitting parameters, we get the frequency of LO (E_1) as $\omega_{\mathrm{LO}}/2\pi = 599$ cm^{-1} (17.98 THz). Compared to the reported experimental value 591 cm^{-1},[12] such a theoretical estimation is reliable. Meanwhile, the TO and LO response process can be represented by the calculated terahertz dispersion curves. As shown in Fig. 4, the dispersion curves for ZnO in the terahertz region are determined by calculating the function, $k_r = 2\pi n_r\omega$ and $k_i = 2\pi n_i\omega$. The real part of wave vector k_r denotes the wave propagation in crystal, while the imaginary part k_i shows the absorption during the process of propagation. It can be seen from the curves that there exist two main propagation branches for $\omega < \omega_{\mathrm{TO}}$ and $\omega > \omega_{\mathrm{LO}}$. An attenuation appears when $\omega_{\mathrm{TO}} < \omega < \omega_{\mathrm{LO}}$. The strong absorption peak corresponds to the TO resonance when frequency ω equals ω_{TO}.

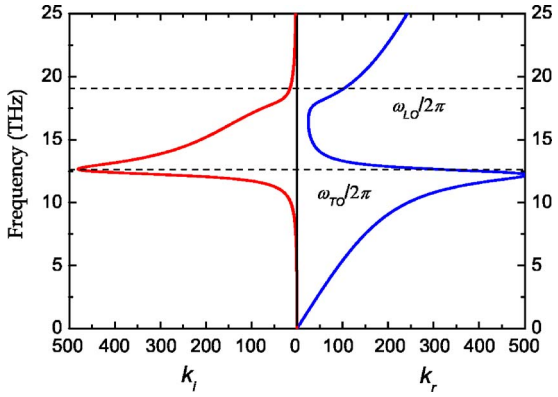

FIG. 4. (Color online) Dispersion relations for ZnO displayed as a function of the real and the imaginary part of the wave vector k. The dashed curves denote the TO and LO phonon resonances.

The authors acknowledge D. Grischkowsky and X. C. Xie for fruitful discussions. This work was partially supported by the Oklahoma EPSCoR for the National Science Foundation, and Oklahoma State University. One of the authors (J.H.) acknowledges the hospitality and financial support of Professor K. Nasu at the Institute of Materials Structure Science, High Energy Accelerator Research Organization, Japan.

[1] V. Srikant and D. R. Clarke, J. Appl. Phys. **83**, 5447 (1998).
[2] Z. K. Tang, G. K. L. Wong, P. Yu, M. Kawasaki, A. Ohtomo, H. Koinuma, and Y. Segawa, Appl. Phys. Lett. **72**, 3270 (1998).
[3] D. M. Bagnall, Y. F. Chen, Z. Zhu, T. Yao, S. Koyama, M. Y. Shen, and T. Goto, Appl. Phys. Lett. **70**, 2230 (1997).
[4] N. Ashkenov, B. N. Mbenkum, C. Bundesmann, V. Riede, M. Lorenz, D. Spemann, E. M. Kaidashev, A. Kasic, M. Schubert, M. Grundmann, G. Wagner, H. Neumann, V. Darakchieva, H. Arwin, and B. Monemar, J. Appl. Phys. **93**, 126 (2003).
[5] D. C. Look, D. C. Reynolds, J. W. Hemsky, R. L. Jones, and J. R. Sizelove, Appl. Phys. Lett. **75**, 811 (1999).
[6] I. H. Lee, K. J. Yee, K. G. Lee, E. Oh, D. S. Kim, and Y. S. Lim, J. Appl. Phys. **93**, 4939 (2003).
[7] S. Ono, H. Murakami, A. Quema, G. Diwa, N. Sarukura, R. Nagasaka, Y. Ichikawa, E. Oshima, H. Ogino, A. Yoshikawa, and T. Fukuda, in *Proceedings of CLEO' 2005*, 22–27 May 2005, Baltimore, MD, Paper No. CThX6.
[8] A. K. Azad, Y. Zhao, and W. Zhang, Appl. Phys. Lett. **86**, 141102 (2005).
[9] L. Thamizhmani, A. K. Azad, J. Dai, and W. Zhang, Appl. Phys. Lett. **86**, 131111 (2005).
[10] W. Zhang, A. K. Azad, and D. Grischkowsky, Appl. Phys. Lett. **82**, 2841 (2003).
[11] M. Balkanski, in *Optical Properties of Solids*, edited by F. Abelès (North–Holland, New York, 1972), Chap. 8.
[12] *Physics of II-VI and I-VII Compounds, Semimagnetic Semiconductors*, edited by O. Madelung (Springer, Berlin, 1982), Chap. 3.
[13] C. A. Arguello, D. L. Rousseau, and S. P. S. Porto, Phys. Rev. **181**, 1351 (1969).
[14] T. C. Damen, S. P. S. Porto, and B. Tell, Phys. Rev. **142**, 570 (1966).
[15] S. S. Mitra and R. Marshall, in *Proceedings of the International Conference on the Physics of Semiconductors* (Academic, New York, 1965), p. 1085.
[16] R. J. Collins and D. A. Kleinman, J. Phys. Chem. Solids **11**, 109 (1959).
[17] F. Decremps, J. Pellicer-Porres, A. M. Saitta, J.-C. Chervin, and A. Polian, Phys. Rev. B **65**, 092101 (2002).
[18] J. M. Calleja and M. Cardona, Phys. Rev. B **16**, 3753 (1977).
[19] R. Loudon, Adv. Phys. **13**, 423 (1964).